Mon. Not. R. astr. Soc. (1983) **204**, 743–763

Abundance gradients in galaxies in the Sculptor and Centaurus groups

B. Louise Webster *School of Physics, University of New South Wales, Kensington, NSW, Australia and Anglo-Australian Observatory, Epping, NSW, Australia*
Malcolm G. Smith★ *Anglo-Australian Observatory, Epping, NSW, Australia*

Received 1982 November 15; in original form 1982 July 20

Summary. About 80 H II regions have been observed spectrophotometrically over the faces of the Sculptor galaxies NGC 55, 253, 300 and 7793 and the Centaurus galaxies M83 and NGC 5253. Radial gradients in the O/H ratio have been measured.

NGC 55 has a zero gradient, a mean oxygen abundance identical to that of its morphological counterpart, the LMC, but a low nitrogen-to-oxygen ratio. The hotspots in NGC 5253 have the low abundance appropriate to the absolute magnitude and mass of the underlying elliptical. The other spirals have marked gradients with a considerable range in mean abundance from one spiral to another. A relation between the oxygen abundance at a characteristic radius and the surface brightness of stars at the same radius is suggested and the implication for galactic evolution is pointed out.

1 Introduction

A powerful tool in understanding the evolution of galaxies and the past history of star formation within them is the study of the chemical evolution of their stars and gas. A comprehensive review of the many facets of the abundance work has been given recently by Pagel & Edmunds (1981). Among elliptical and S0 galaxies there is, broadly speaking, a relation between metal abundance and the absolute magnitude of the system and also, in the more luminous galaxies, a radial change in abundance. Late-type spiral galaxies generally show radial gradients in O/H, but no clear trend with morphological type or any other property has yet emerged. The gassy irregulars and related dwarfs conform most closely to a simple model of galactic chemical evolution since they obey a simple relation between the heavy element content and the ratio of the mass of the system to the mass of residual gas. In this paper we study H II regions in six late-type spiral and irregular galaxies and find some evidence for a relation between oxygen abundance and the surface brightness of the stellar component.

★Present address: Royal Observatory Edinburgh, Edinburgh, Scotland.

The existence of radial abundance gradients in H II regions in spirals was first demonstrated by Searle (1971) and subsequent work has firmly established the fact that the abundance of oxygen relative to hydrogen decreases outwards in many late-type galaxies. The evidence for radial variations of one heavy element relative to another is not strong. Furthermore, a positive O/H gradient is accompanied by a softening of the ionizing radiation caused either by the increased metal opacity in the atmospheres of the exciting stars (Balick & Sneden 1976), by a change in the initial mass function (the formation of massive stars may be impeded, Shields & Tinsley 1976) or by increased dust which selectively absorbs the ionizing radiation (Sarazin 1976). The combined effect of a lower electron temperature in higher abundance objects (Searle 1971) and the modification of the radiation field produces very striking changes in the emergent spectra of the H II regions and if it can be established

Table 1. Galaxy parameters.

Galaxy	NGC 55	NGC 253	NGC 300	NGC 7793	NGC 5236 (M83)	NGC 5253
Type	SB(s)m	SAB(s)c	SA(s)cd	SA(s)dm	SAB(s)c	Irr IIp
l^{II} (°)	332.8	97.6	299.2	4.5	314.6	314.9
b^{II} (°)	−75.7	−88.0	−79.4	−77.2	32.0	30.1
Distance modulus	26.8[2]	27.0[3]	26.5[2]	27.5[2]	27.84[4]	27.1[4]
Distance (Mpc)	2.3	2.5	2.0	3.2	3.7	2.6
α (°)	105[5]	51[3]	109[6]	108[7]	45[1]	–
i (°)	85[5]	78[3]	42[6]	53[7]	24[1]	–
ρ_0 (arcmin)	11.5[1]	9.8[3]	9.8[1]	4.4[1]	5.9[1]	1.8[1]
log $(M/M_\odot)$	10.5[5]	11.2[3]	10.3[6]	9.9[8]	10.9[9]	9.7[10]
M_H/M_{total}	0.18[11]	0.02[11]	0.11[11]	0.08[8]	0.03[11]	0.04[10]

References

1. RCBG2, de Vaucouleurs *et al.* (1976).
2. de Vaucouleurs (1982 private communication. (A lower value of about 26.4 or less has recently been suggested for NGC 55 and 300 by Graham 1982.)
3. Pence (1978).
4. de Vaucouleurs (1979).
5. de Vaucouleurs & Freeman (1972).
6. de Vaucouleurs & Page (1962).
7. de Vaucouleurs & Davoust (1980).
8. Davoust & de Vaucouleurs (1980).
9. Rogstad, Lockhart & Wright (1974).
10. Bottinelli, Gouguenheim & Heidmann (1972).
11. Roberts (1975).

that the radiation field in a giant H II region is uniquely related to the O/H ratio then quite straightforward observations can give information on the oxygen abundance. Our interpretation of the observations does rely heavily on this assumption but in half the galaxies studied it can be checked by an 'exact' analysis.

The galaxies studied are four in the nearest group to our own, the Sculptor group, and two in the Centaurus group and they are listed, with some of their properties, in Table 1. Other studies of abundances in their H II regions, carried out while our work was in progress, are referenced. We have chosen bright H II regions at a range of distances from the galactic nucleus. The nebulae are identified in Plates 1–3.

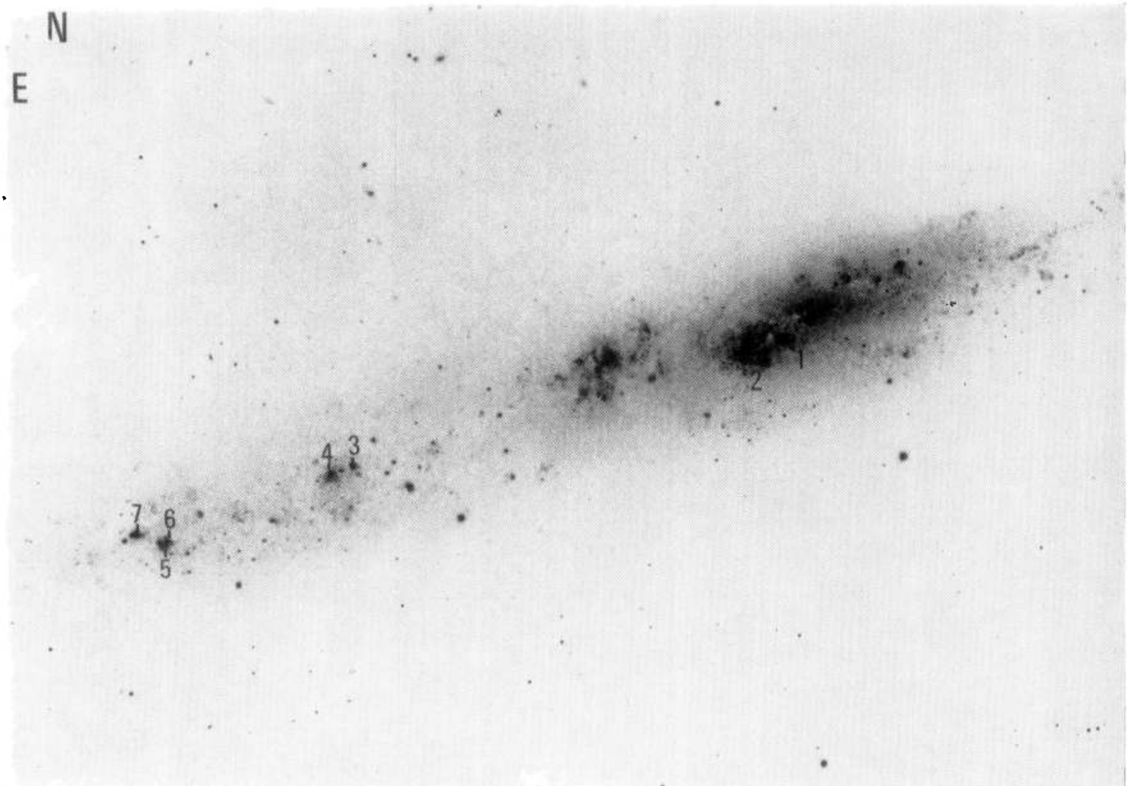

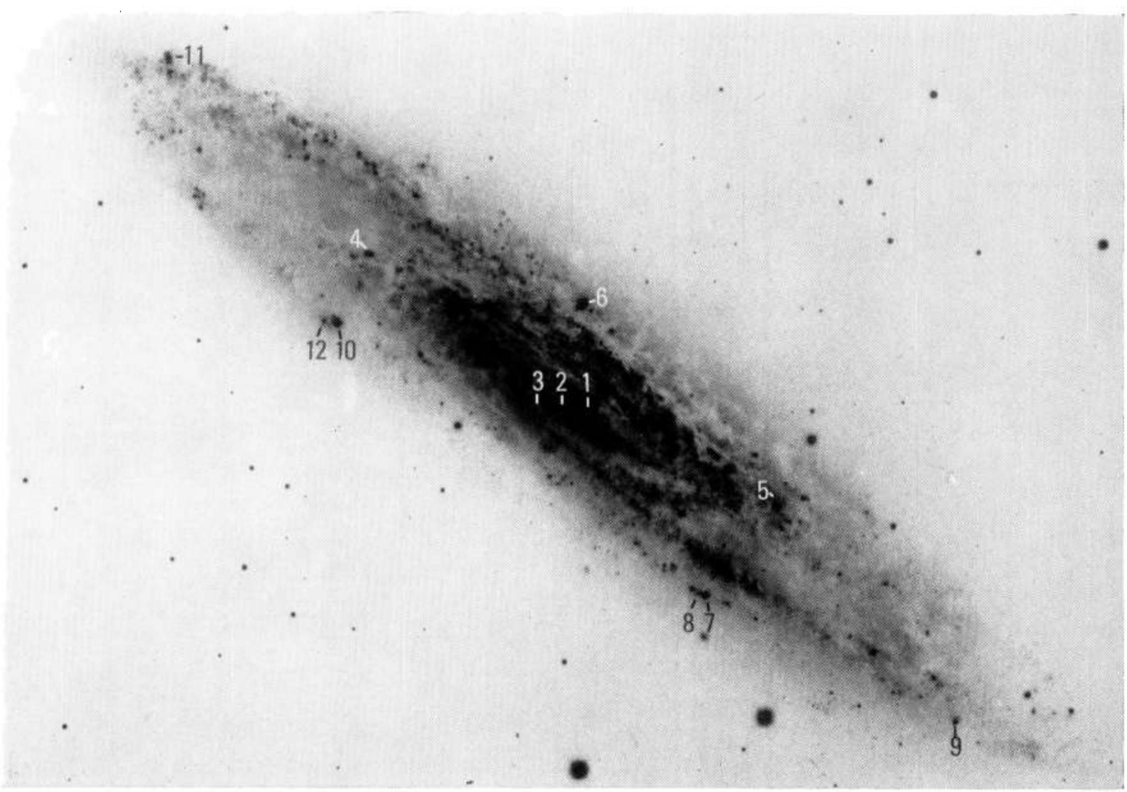

Plate 1. Top: H II regions in NGC 55. The four photographs in Plates 1 and 2 are reproduced from a matched set of Hα plates taken at the prime focus of the CTIO 3.9-m telescope (098 − 02 emulsion, Hα filter, 45-min exposure). The first five photographs have the same linear scale; each measures 14 kpc by 9.7 kpc. Bottom: H II regions in NGC 253.

[*facing page* 744]

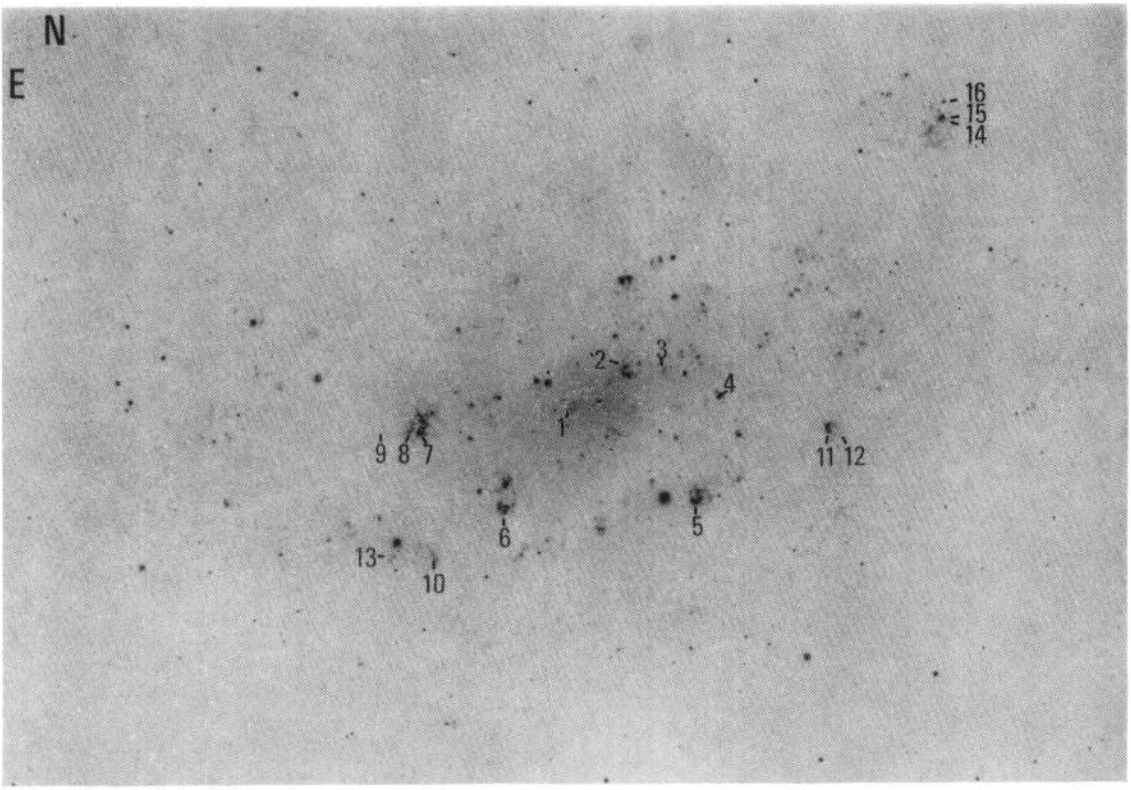

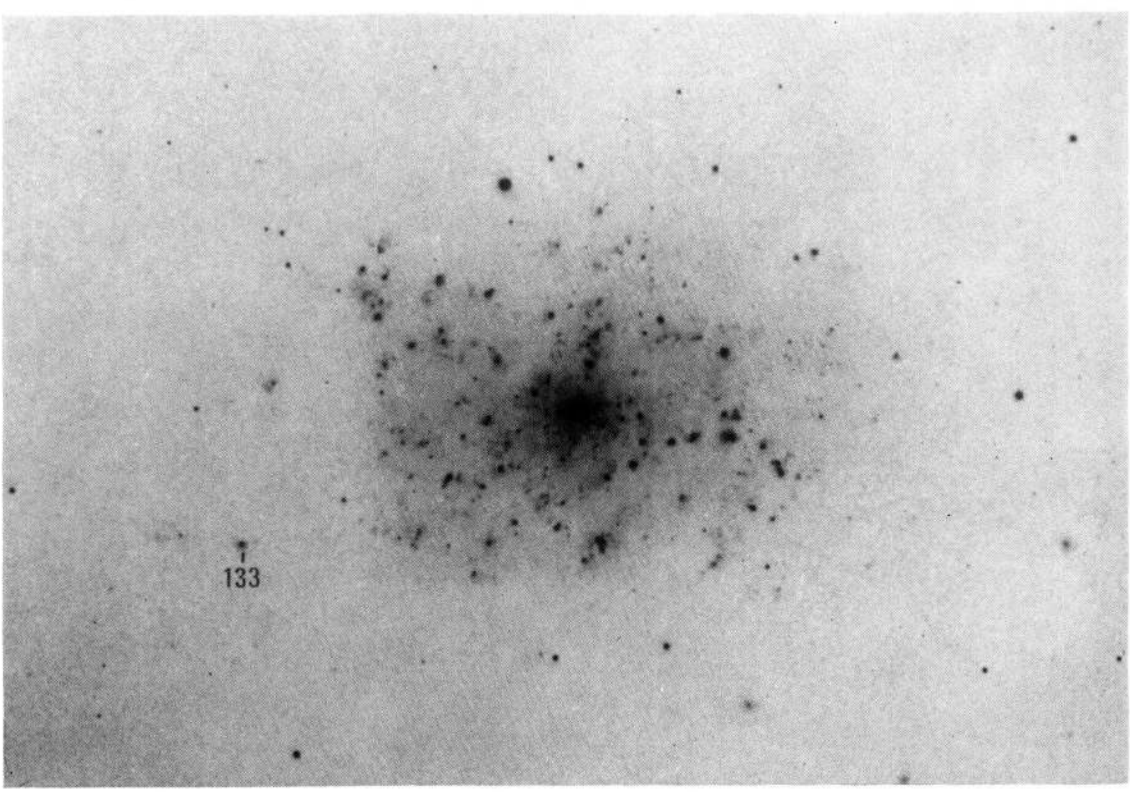

Plate 2. Top: H II regions in NGC 300 (see caption to Plate 1). Bottom: H II regions in NGC 7793. Only region 133 is marked; the others are identified by Davoust & de Vaucouleurs (1980).

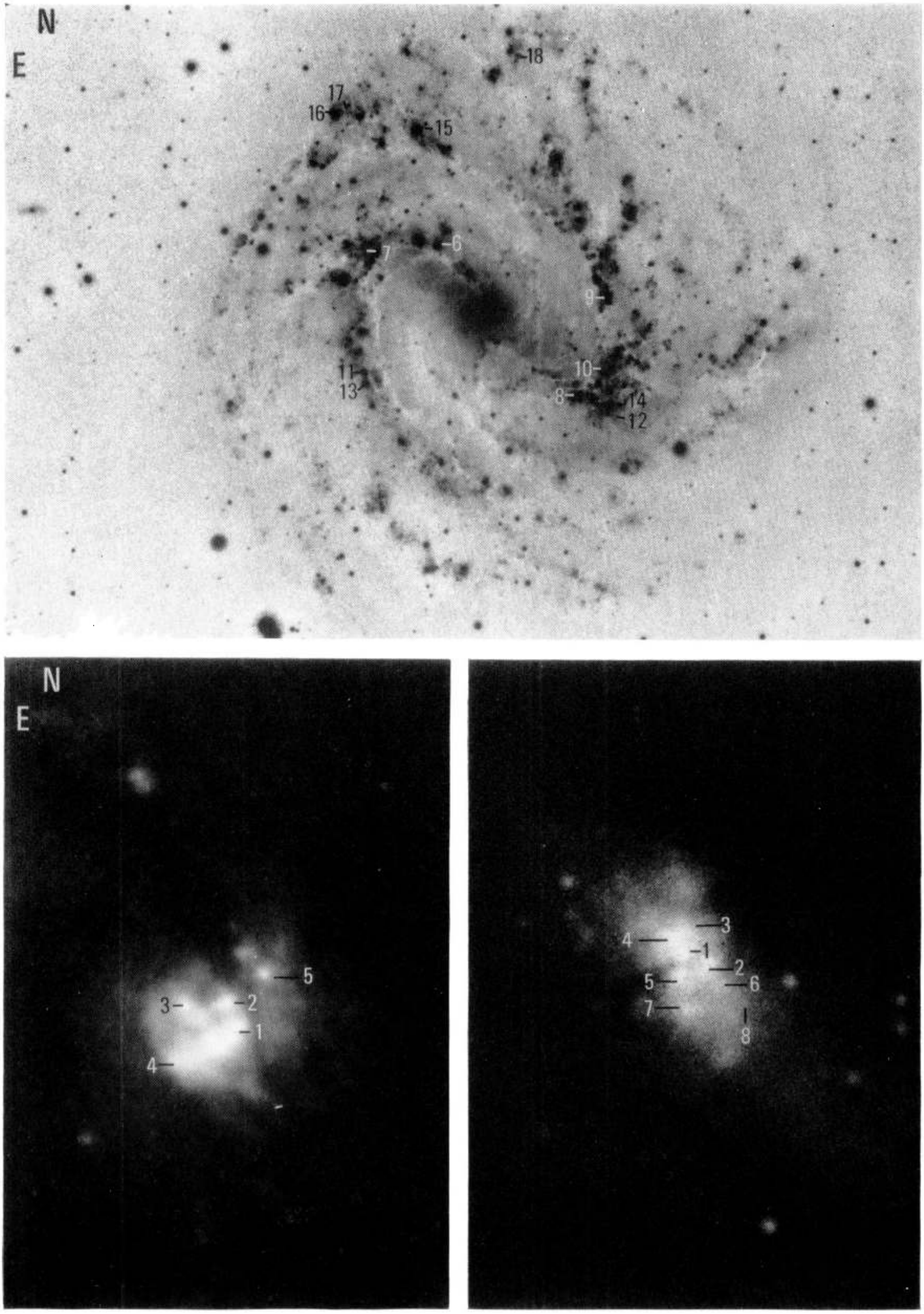

Plate 3. Top: H II regions in NGC 5236 (M83). From a panchromatic photograph taken with the 3.9-m AAT by D. Malin. Bottom left: enlargement of the central region of NGC 5236. Bottom right: the H II regions in NGC 5253. From a blue photograph taken with the 3.9-m AAT.

2 Observations

2.1 OBSERVATIONAL PARAMETERS, PROCEDURE AND REDUCTIONS

The spectrophotometry reported here was obtained between 1975 and 1977 with the Anglo-Australian telescope on Siding Spring mountain. Two instrumental systems were used, the

Table 2. Observing parameters.

Code	AP	WD	BD	RD
Spectrograph	RGO	B&C	B&C	B&C
Detector	IPCS	IDS	IDS	IDS
Wavelength region (Å)	3400–7400	3650–7300	3600–5300	5700–7400
Resolution (Å)	13	10–20	8	8
Slit width (arcsec)	2	1.8	1.8	1.8
Slit length (arcsec)	18 × 4.7	4.5	4.5	4.5

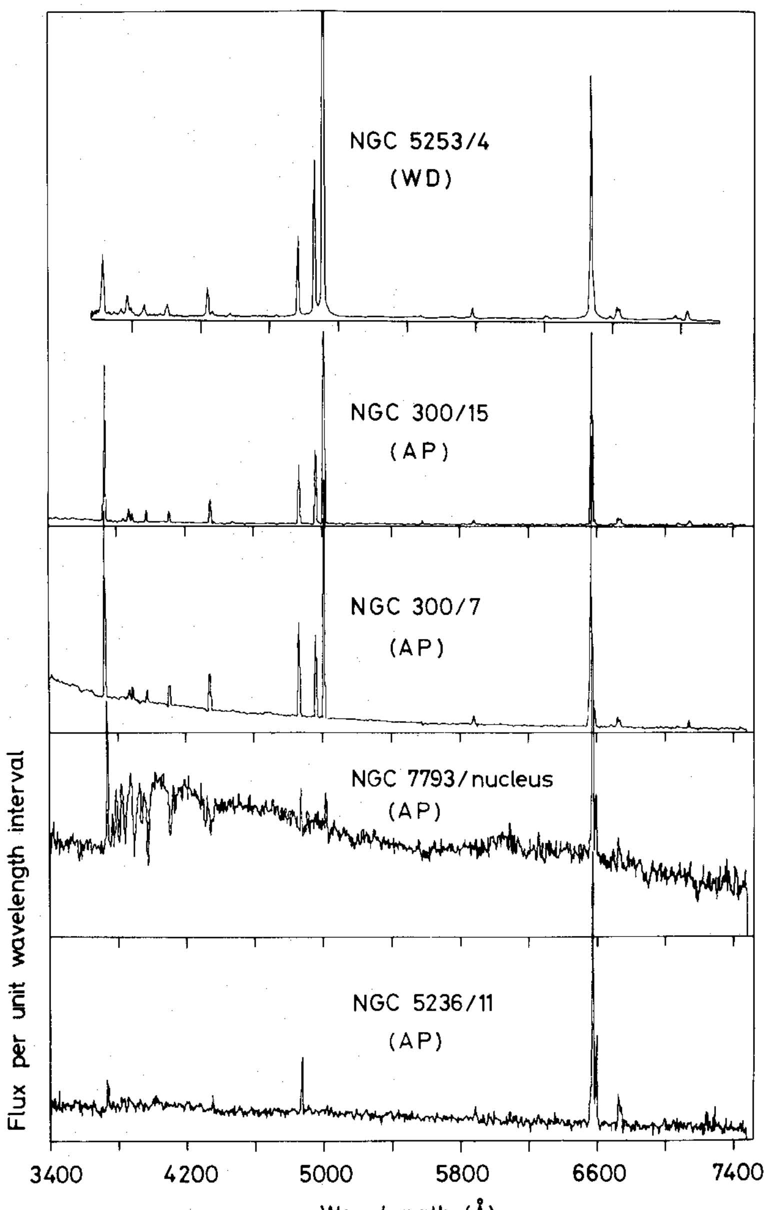

Figure 1. Examples of spectral scans. Each scan is plotted at a different flux scale. The letters below each H II region identification refer to the observing code (Table 2).

Boller and Chivens Cassegrain spectrograph with the Wampler–Robinson image dissector scanner (IDS) and the RGO spectrograph with the Boksenberg image photon counting system (IPCS). The observing parameters are summarized in Table 2, and examples of spectral scans are shown in Fig. 1.

With the IPCS system (code AP) the 84-arcsec slit was divided into 18 spatial increments perpendicular to the dispersion, while 990 spectral increments along the dispersion gave a spectral resolution sufficient to resolve all the close line pairs of interest except the [O II] 3726/29 doublet. Each H II region was observed at least twice, first towards one end of the slit, then towards the other end. During reductions all increments along the slit with appreciable contributions of emission from the nebula were added (usually about three increments) and sky subtracted by using an equal number of increments, where possible from the part of the slit where the nebula was located in the complementary observation. For the brighter nebulae the procedure was carried out both without and with a neutral density filter to keep the strong lines below the saturation level of 1 Hz. Sensitivity calibration was made by observing white dwarf standards (Oke 1974) with the slit width much wider than the seeing disc.

Three set-ups were used with the image dissector system (IDS). The most frequent was one (code WD) covering the spectrum from the short wavelength system cut-off to about 7200 Å with a resolution just sufficient to resolve the close line pairs (not [O II] 3727). Occasionally higher resolution in the blue (code BD) or red (code RD) was employed, see Table 2. The sensitivity of the detector was very low at wavelengths shorter than about 4300 Å. The two entrance apertures were 4.5×1.8 arcsec on the sky separated by 20 arcsec. The observing procedure was the standard one of measuring each H II region first in one aperture, then in the other, the opposite aperture in each case being used for sky subtraction. When the opposite aperture was contaminated by emission or a bright star the telescope was moved and the sky measured in both windows. Sensitivity calibration was again obtained from Oke white dwarfs, but with the same entrance apertures.

The observations were reduced using the AAO reduction package SDRSYS written by J. Straede. The two spectra of each object at different positions on the slit were reduced separately and combined later, except for faint noisy lines. Though this doubled the work it allowed a more realistic estimate of the accuracy to be made.

The IPCS line intensities were measured both by adding counts above the continuum in the appropriate channels and by fitting Gaussian profiles. The IDS intensities were measured by fitting a profile which was a mixture of Gaussian and Lorentzian with the proportion of each and the FWHM chosen at each wavelength on each night by fits on the comparison arc and on bright nebular lines (the SDRSYS program PROFIL). Both isolated and blended lines could be measured accurately in this way.

2.2 RESULTS AND ACCURACY

The line intensities have been corrected for reddening by assuming a true $H\alpha/H\beta$ ratio of 2.86 which is given by Brocklehurst (1971) for $T_e = 10^4$ K. For many regions $T_e = 5000$ K ($H\alpha/H\beta = 3.03$) is more appropriate, but the difference is small and the former value has the advantage of being widely used. The Miller–Mathews formula (1972) for the Whitford reddening curve was adopted. The line intensities are listed in Table 3 relative to $H\beta = 100$ (or $H\alpha = 286$ if $H\beta$ was not available).

To some extent the two instrumental systems are complementary. The IDS plus B&C spectrograph can work to higher intensities and was better for the relative intensities of lines close together in the spectrum. This is demonstrated by the value of [O III] 5007/

4959 = 2.95 found in this and other series of observations, whereas the IPCS gives a value systematically about 10 per cent too high. IDS intensities have no claim to accuracy over the whole spectrum. First, this particular dissector slit (6 arcsec) is close in size to the spectrograph entrance aperture (4.5 arcsec) and small deviations in the sweep pattern or position of the object lead to variation in the signal. Secondly, the slit could not be conveniently widened for the standard stars. Since most important lines are close to Balmer lines this only means that the dissector observations cannot be used for determinations of the reddening parameter c (Hβ) or for accurate 3727 intensities where, also, the instrumental sensitivity is very low. The IPCS plus RGO spectrograph has a cleaner profile and is better for relative intensities over the whole wavelength range (though see comparison with Pagel below). The two-dimensional mode was particularly useful for obtaining spatial information on the line intensities.

Most of the observations reported here were made in a four-night run in 1977 August, including essentially all of our observations of the Sculptor group H II regions. The Centaurus regions in M83 and NGC 5253 were observed on 1¼ nights in 1976 March and several were re-observed in 1977 August for comparison and as calibration. Other IDS observations were made sporadically through 1975–76 and give valuable additional information on faint lines.

The error in each line intensity relative to the Balmer lines was estimated from consideration of photon noise and inter-agreement between the double measurement and between different scans. An error code has been assigned where a = < 10 per cent, b = 10–20 per cent,

Table 3. (a) NGC 55: line intensities corrected for reddening relative to Hβ = 100. The letters are error codes (see text).

Ion	Nebula λ	1	2	3	4	5	6	7
[O II]	3727	170a	266c	524b	706c		478b	261a
H10	3797	2.9c		4.4c				
H9	3835	7.0c		6.2c				3.2c
[Ne III]	3868	40c	29c	16c			29c	37c
H8 + He I	3889	21c	18c	19c			14c	17c
Hδ	4101	24.3b	21.0c	28.5b			21.8c	23.3c
Hγ	4340	43.4b	39.8b	49.4b			47.9c	44.4b
[O III]	4363	3.9c	3.2c	1.2c			≲8.7d	3.3c
He I	4471	2.8b	3.6c	4.0c				3.4c
Hβ	4861	100a	100b	100a	100c	100a	100b	100a
[O III]	4959	172a	147b	72b	63c	132a	87b	142a
[O III]	5007		445b	236b	203b	383a	286b	441a
He I	5876	10.1b	9.5c	7.2b			14.5c	9.9b
[O I]	6300	2.3d	3.1c					
[S III]	6312	2.0d	1.5c					
Hα	6563	286a	286a	286a	286c	286c	286a	286a
[N II]	6584	6.6b	9.0c	18.0c	14d	15c	17.2c	10.6c
He I	6678	2.5c	2.8c	1.6c				3.5d
[S II]	6717	6.7b	10.7b	19.0c	45c	17.8c	42c	12.2c
[S II]	6731	5.7b	7.9b	13.8c	28c	9.9c	24c	9.7c
He I	7065	2.3c	3.4c					
[Ar III]	7136	9.3c	14.0c	5d				6.8b
c (Hβ)		0.44	0.24	0.47	0.45	0.26	0.26	0.34
Code		AP, WD, BD, RD	WD, BD, RD	AP, 2BD 2RD	AP	WD, 2BD 2RD	AP	AP, 2BD, 2RD
Remarks				6		1		6

Table 3 – *continued*

(b) NGC 253: line intensities corrected for reddening.

	Nebula	1	2	3	4	5	6	7	8	9	10	11	12
Ion	λ				153b	245b	349a	321a	220c	409b	260b	361b	251c
[O II]	3727												
H9	3835						5.9c						
[Ne III]	3868						3.6b						
H8 + He I	3889						16.8b	26c					
Hδ	4101						29.6b	30.1c					
Hγ	4340				43.8c		50.7a	57.2b		66d	43.1b	55.7c	
He I	4471						3.3c						
Hβ	4861	100d			100b	100b	100a	100a	100b	100c	100b	100b	100c
[O III]	4959						30a	30.6b			23c	54b	35c
[O III]	5007				⩽18	45c	98a	104b	62c	49c	71c	167b	74c
He I	5876						8.2b	6.3c			9.5c	9.8c	
[N II]	6548	67b	111c	116d			16c				31c		
Hα	6563	286a	286c	286d	286a	286b	286b	286a	286b	286b	286b	286b	286c
[N II]	6584	80a	289c	311d	71c	73c	56b	61c	84c	86c	76b	46c	57c
[S II]	6717	52.2b	160d		84c		19.6b	21.3b		61c	20.1c	15.5c	
[S II]	6731	35.7b					12.0b	13.4b			22.2c	12.0c	
C(Hβ)		2.43:	–	–	0.74	0.46	0.58	0.92	0.21	0.82	0.82	1.06	0.26:
Code		AP	AP	AP	AP	AP	AP	AP	AP	AP	AP	AP	AP
Remarks		5	2	2			12,6						

Table 3 – *continued*

(c) NGC 300: line intensities corrected for reddening.

Ion	λ	Nebula 1	2	3	4	5	6	7	8	9	10	11	12	13	14	15	16
[O II]	3727	236b	449a	374c	418a	394b	168d	223b	238a	1280c	181b	337a	499b	329c	213a	290a	339b
[Ne III]	3868							12.9b	22c			20.7c			32c	28.6b	
H8 + He I	3889				16.3c			15.7b	11.3c			15.1c			15.8c	17.6b	
Hε + [Ne III]	3967				15.4c										21c	23.9b	
Hδ	4101		24.6b		22.5b	22.4c	7.5d	24.0b	21.7b			19.5b			22.1b	25.6b	26.4c
Hγ	4340	44.0c	43.2b		49.7a	45.7b	37b	47.7a	41.5b			44.9a	52.4c		43.4b	47.9a	44.1b
[O III]	4363					<1.7		0.66c	<2.9			⩽1.1				4.4c	
He I	4471						4.0c	3.4c	<3.2			2.5d				3.5c	
Hβ	4861	100b	100a		100a	100a	100a	100a	100b		100b	100a	100b	100c	100a	100a	100b
[O III]	4959				13.7b	60a	54a	81b	72b		159a	73b	52c		136b	126a	86b
[O III]	5007	34c	41b		37b	179a	153a	242b	220b		437a	213b	170b		490b	430a	281b
He I	5876					10.1b		9.7b	13.7b			8.6c					
Hα	6563	286b	286a	286c	286a	286a	286a	286a	286a	286d	281a	286a	286b	191c	286a	286a	286a
[N II]	6584	54c	63b		46c	32.8b	33b	16.6c	25c		32d	31.0b	24d		7d	12.4c	8d
He I	6678					1.3d	3.2d	2.4d								2.8c	
[S II]	6717	47c	84.2a		42.6b	19.6c	20.4b	9.9b	15.4b			26.9b	51c		59c	18.2b	29d
[S II]	6731	27c	55.8a		30.4b	15.8c	16.4b	6.3c	12.3b			21.7b	49c			11.9b	
[Ar III]	7135					8.7d		6.9c								7.4d	
C(Hβ)		0.37	0.28		0.33	0.34	0.18	0.30	0.29		0	0.12	0.26	0	0.13	0.14	0.21
Code		AP	AP, BD, RD	AP	AP, BD, RD	AP, WD, BD, RD	WD, BD, RD	AP, 2BD, RD	AP	AP	AP	AP, WD, BD, RD	AP	AP	AP	AP	AP
Remarks				2		13, 18		7, 14	6	2		15			8	6, 8	

Table 3 – *continued*

(d) NGC 7793: line intensities corrected for reddening. (Identifications from Davoust & de Vaucouleurs 1980.)

Ion	Nebula λ	Nucleus	Nucl.W.	23	33	36	44	25	25N	26 + 19
[O II]	3727	273c	211c	242c	272c	349b	300c	270a	353b	313c
H 8 + He I	3889					17.7c				
Hε + [Ne III]	3967					9.9c				
Hδ	4101					30.7c		21.4c	33.7c	
Hγ	4340			50.3c	38.6c	47.7b		44.4b	52.8b	
Hβ	4861	40d	100c	100c	100c	100b	92d	100a	100b	112d
[O III]	4959					44b		31.5b	29c	
[O III]	5007	58d	41d	31d	36c	163b	71d	111a	112b	67d
He I	5876					11.2c		15.7d		
Hα	6563	286c	350c	341b	256b	286a	286c	286b	286b	286c
[N II]	6584	82c	66c	49c	48c	31.8c	55d	39c	38c	48d
[S II]	6717	73d	55d			22c	101d	29.8c	23.5c	96d
[S II]	6731					9.7c		15.3c	19.6c	
C (Hβ)		0.38	0.38	0.38	0.38	0.61	0.38	0.26	0.30	0.3
Code		AP	AP	AP	AP	AP	AP	AP	AP	AP
Remarks		3,4	3	3	3					3

Table 3 – *continued*

(e) NGC 5236: line intensities corrected for reddening.

Ion	Nebula λ	1	2	3	4	5	6	7	8
[O II]	3727		41c		(93)	133d			≲200
Hδ	4101		28.7c						
Hγ	4340		44.3b			39.1d			
Hβ	4861	100c	100c			100c	100b		100b
[O III]	4959								
[O III]	5007		7.3b			12c	≲10		≲15
He I	5876		6.6c						
Hα	6563	286b	286b	286c	286c	286d	286b	286b	286d
[N II]	6584	198c	140b	177c	144c	119c	97c	97c	112c
[S II]	6717	53b	18.3b	58c	62c	32b	17.6c	70c	91c
[S II]	6731	58b	21.9b	59c	48c	29b	16.9c		
C (Hβ)		0.60	0.79		0.60	0.96	0.50		0.
Code		WD	AP, 2WD	WD	WD, (AP)	AP, WD	WD	WD	WD
Remarks		4	4	2, 4	1,4	4		2,10	

	20S	13	13 S1	13 S2	10	39	4	2	1	133
)	272b	451b	308b	423b	421b	251c	644c	430b	288d	293b
					21.8c					28c
2b	38.6c	52.5b		49.0c	43.6b			52.2b	45.0c	40.3c
)	100c	100b	100c	100b	100b	100c	98d	100b	100b	100b
)	12c	27b		27c	24c			50b	34c	77b
)	36c	85b	51c	71b	69b	24d	159c	187b	113b	251b
					8.7d			11.5c		
)	185b	286b	204c	286b	286b	317c	286c	286b	286b	286a
:	32c	44c	66c	48c	35c	58d		32c	≤15	≤13
5c	25c	35.5c	76d	42c	29.2c			22.7c	48c	
1c		28.3c		24c	20.1c			16.6c		
39	0.38	0.53	0.38	0.51	0.19	0.38	0.38	0.34	0.47	0.18
	AP	AP	AP	AP	AP	AP	AP	AP	AP	AP
	3		3			3	3			9

	10	11	12	13	14	15	16	17	18
0									
	168d	93d	≲390	178b	≲210		200b	118d	
	31c						44.6c		
0b	100b	100c	100c	100b	100c	100b	100b	55d	100c
							25b		
0	18c	< 9	≲30	20c	<30	13d	87b	<10	<30
							12.9b		
6b	286d	286b	286c	286a	286c	286b	286a	286b	286c
1c	143c	92c	123d	107c	174d	117c	118c	99c	125d
9c	36c	57c	82c	27c	99d	60c	40b	58c	100d
5c	27c			23c		32c	29b	21c	
0.50	0.36:	0.79	0.39	0.75	0.06	0.13	0.18	0.18	–
	2WD	AP, WD	WD	AP, WD	WD	WD	AP, WD	AP	WD
						10		1	2

Table 3 – *continued*

(f) NGC 5253: line intensities corrected for reddening.

Ion	Nebula λ	1	2	3	4	5	6	7	8
[O II]	3727	198d	391d	123d	149d	343d	367c	230d	717c
H9	3835	8.7d		2.2d	5.7c				
[Ne III]	3868	39d		42d	48c	28d			
H8 + He I	3889	23d		14d	16c	5d			
Hδ	4101	18.2c		20.6c	20.4b	9.4c		18.4d	
Hγ	4340	41.0b	37.5c	44.5b	43.3a	41.3b	40.0c	44.9b	
[O III]	4363	3.9c		7.5b	6.7b	3.6d			
He I	4471	3.2c		3.9b	3.7b	2.3d			
Hβ	4861	100a	100b	100a	100a	100a	100b	100b	100c
[O III]	4959	144a	95b	215a	201a	114a	114b	124a	146b
[O III]	5007	442a	319a	631a	581a	348a	359b	403a	357b
He I	5876	11.9b	8.0c	13.3b	12.2b	10.4b		13.0c	
[O I]	6300	3.6c	8.7c	2.6c	2.3b	6.0c			
[S III]	6312	1.4c		2.5c	2.2b				
[O I]	6363	1.5d		0.7d	0.7c				
Hα	6563	286a	286a	286a	286a	286a	286a	220b	286b
[N II]	6584	17d	20.8d	25d	19d	23d	21d	15d	
He I	6678	4.1c		3.7b	3.3c				
[S II]	6717	25.0b	37.6b	13.6b	11.6b	39.1b	31.1b	31.8c	54c
[S II]	6731	19.3b	25.6b	13.3b	10.8b	29.1b	24.1b	19.1c	
He I	7065	3.5c		6.1b	5.3b				
[Ar III]	7135	11.4c	<7	13.8b	11.7b	8.6c		8.3d	
C (Hβ)		0.13	0.31	0.23	0.38	0.11	0.38	0	0.84
Code		WD	WD	WD	2WD	WD	AP, WD	WD	AP
Remarks		6	6	6	6, 17	6	6	6	4

Notes

1. Reddening assumed to be the same as the neighbouring nebula.
2. Normalized to Hα = 286, with zero reddening.
3. Reddening assumed to be the average of the galaxy.
4. Strong continuum.
5. Strong red continuum.
6. Strong blue continuum.
7. Nebula 7 = W21, Pagel *et al.* (1979).
8. Nebulae 14 and 15 are different parts of No. 7, Pagel *et al.* (1979).
9. Nebula is outside the survey of Davoust & de Vaucouleurs (1981). The number is a continuation of their catalogue.
10. Nebula 15 = No. IV Dufour *et al.* (1980). (They quote 'insufficient observations'.)
11. Nebula 9 = No. III Dufour *et al.* (1980).
12. λ 6678 = 1.6c, λ 7135 = 4.5c.
13. λ 6300 = 3.2d.
14. Blue continuum. Broad 4686 ~ 12 from Wolf–Rayet star/s.
15. Blue continuum. Broad 4686 ~ 7 from Wolf–Rayet star/s.
16. λ 4363 $\lesssim$ 5.
17. λ 4068 = 2.9d, λ 4076 = 1.4d, λ 4658 = 1.2d, λ 4712 = 1.7c, λ 4740 = 1.0d.
18. Nebula 5 = No. 5 Pagel *et al.* (1979).
19. C (Hβ) = $\log_{10}$ (true Hβ intensity)/(observed Hβ intensity).
20. Code. AP = Full wavelength coverage, photon counting. WD = Full wavelength coverage, image dissector scanner. BD, RD = Blue and red spectral regions, image dissector scanner.

c = 20–40 per cent and d = > 40 per cent. Calibration errors are not explicitly included, but would only affect the values of c (Hβ) and [O II] 3727 as mentioned earlier.

A comparison was possible for three regions in NGC 300 with Pagel *et al.* (1979). We derive a much lower reddening for NGC 300 than they do (ours is probably one that is more appropriate to the galactic latitude of this galaxy), but otherwise the comparative intensities are well within the quoted errors. The one exception is Nebula 14/15 where a difference of 25 per cent in the well-observed [O III] lines clearly reflects the fact that our observations have been made at a different part of this extended region. A comparison was attempted with Dufour *et al.* (1980) in M83. Their nuclear region appears to correspond to our Nebula 5 but their much larger entrance slot leads to a much higher reddening and to stronger [N II]. We have only sketchy observations of their region III (Nebula 9) but the agreement is satisfactory. Two additional lightly reddened H II regions were observed in 1977 August, IC 1644 in the Small Magellanic Cloud and Tololo 1924–416. In each of these the observed Balmer decrement is close to the theoretical one implying small reddening, as is expected, so we have some confidence in our calibration.

3 Abundance analysis

Abundances of the heavy elements can be derived in two ways. In nine H II regions (about 10 per cent of the total) the temperature dependent [O III] 4363/5007 + 4959 ratio has been measured and the O^{++}/H^+ value can be derived directly (e.g. Osterbrock 1975). If it is assumed that the nebula is isothermal, the abundances of other ions can be calculated from a single line strength each. In most of our nebulae the [O III] 4363 line is too weak to measure and in this case the abundances must be inferred from the strong lines only. In the future we hope to do more detailed modelling of the more interesting nebulae, especially those in the nucleus of M83, but in this paper we have chosen to follow the procedure developed by Pagel *et al.* (1979) and Pagel, Edmunds & Smith (1980), which has been the most convincing of the strong-line methods.

3.1 ABUNDANCES FROM MEASURED T_e

Table 4 lists the ionic abundances of 11 nebulae in which λ4363 has been detected or in which a useful upper limit can be put on its strength. The density can be derived from the ratio [S II] λ6717/6730. Generally the ratio is close to the low density limit in all the accurate cases and the value $N_e = 10^2\,\mathrm{cm^{-3}}$ has been adopted. In some of the central regions of M83, NGC 5253 and possibly NGC 55, collisional de-excitation affects the ratio and densities up to $2\times10^3\,\mathrm{cm^{-3}}$ occur. We have taken $N_e = 10^3\,\mathrm{cm^{-3}}$ when the ratio is 1.0 ± 0.2. The analysis has been the standard one, assuming a uniform temperature distribution (Osterbrock 1975; Pradhan 1976).

Atomic abundances have been calculated from

$$\frac{He}{H} = \frac{He^+}{H^+} \text{ (weighted mean of } \lambda 5876 \text{ and } \lambda 4471)$$

$$O/H = (O^+ + O^{++})/H^+$$

$$N/O = N^+/O^+.$$

These are given in Table 4. For comparison purposes the last column of the Table lists the O/H obtained through the strong-line method to be discussed next. Agreement is moderately satisfactory. It is clear from the more precise values in this section that NGC 55 has a higher O/H abundance than NGC 5253.

Table 4. Abundances in nebulae with temperatures measured from the [O III] lines.

Nebula	N_e	T_e	He^+/H^+	O^o/H^+	O^+/H^+	O^{++}/H^+	N^+/H^+	S^+/H^+	Ar^{++}/H^+	12 + log O/H	log N/O	PES 12 + log O/H
NGC 55												
1	10^3	10340	0.067	2.9E-6	8.3E-5	1.5E-4	1.2E-6	3.9E-7	1.0E-6	8.37	−1.84	8.23
2	10^2	10180	0.072	4.1E-6	1.1E-4	1.4E-4	1.7E-6	5.6E-7	1.6E-6	8.39	−1.81	8.23
3	10^2	9170	0.059	–	3.3E-4	1.0E-4	4.3E-6	1.3E-6	6.8E-7	8.64	−1.88	8.25
7	10^2	10300	0.073	–	9.9E-5	1.3E-4	1.9E-6	6.7E-7	7.6E-7	8.36	−1.72	8.23
NGC 300												
5	10^2	< 11100	0.077	> 3.4E-6	> 1.1E-4	> 4.3E-5	> 4.9E-6	> 9.1E-7	> 8.2E-7	> 8.18	–	8.42
7	10^2	7810	0.067	–	3.0E-4	1.9E-4	6.4E-6	9.2E-7	1.6E-6	8.69	−1.67	8.51
11	10^2	⩽ 9200	0.06:	–	⩾ 2.0E-4	⩾ 9.3E-5	⩾ 7.4E-6	⩾ 2.0E-6	–	⩾ 8.46	–	8.44
15	10^2	11360	0.07:	–	7.2E-5	9.7E-5	1.8E-6	6.5E-7	6.7E-7	8.23	−1.61	8.23
NGC 5253												
1	10^2	10840	0.084	4.1E-6	5.5E-5	1.1E-4	2.6E-6	1.2E-6	1.1E-6	8.23	−1.33:	8.29
3	10^3	12000	0.097	2.3E-6	3.4E-5	1.2E-4	3.2E-6	6.6E-7	1.1E-6	8.19	−1.03:	8.16
4	10^3	11870	0.089	2.1E-6	4.3E-5	1.2E-4	2.5E-6	5.5E-7	9.6E-7	8.20	−1.24:	8.18

Table 5. Nebular parameters and abundances from the strong-line method.

Nebula	ρ/ρ_0	C(Hβ)	[O III]/ Hβ	[O II] + [O II]/Hβ	log [N II]/ [O II]	[N II]/Hα	[S II] 6717/ 6731	PES 12 + log O/H
NGC 55								
1	0	0.44	6.9	8.6	−1.29	0.03	1.18	8.23
2	0.05	0.24	5.9	8.6	−1.35	0.04	1.35	8.23
3	0.53	0.47	3.1	8.3	−1.34	0.08	1.37	8.25
4	0.56	0.45	2.7	9.7	−1.58	0.07	1.61	8.16
5	0.78	0.26	5.2	>5.2	–	0.07	1.79	–
6	0.78	0.26	3.7	8.5	−1.32	0.08	1.79	8.23
7	0.81	0.34	5.8	8.4	−1.27	0.05	1.25	8.23
NGC 253								
1	0.04	2.4:	–	–	–	0.37	1.47	–
2	0.05	–	–	–	–	1.35	–	–
3	0.14	–	–	–	–	1.45	–	–
4	0.45	0.74	<0.2	1.5–1.8	−0.21	0.33	–	9.21–9.28
5	0.49	0.46	0.6	3.1	−0.40	0.34	–	8.87
6	0.66	0.58	1.3	4.8	−0.67	0.26	1.64	8.58
7	0.75	0.92	1.4	4.6	−0.60	0.28	1.59	8.62
8	0.81	0.21	0.8	3.0	−0.29	0.39	–	8.87
9	0.84	0.82	0.7	4.7	−0.55	0.40	–	8.58
10	0.85	0.82	1.0	3.6	−0.41	0.35	0.91	8.77
11	0.92	1.06	2.2	5.8	−0.77	0.21	1.30	8.48
12	0.93	0.26:	1.0	3.5	−0.52	0.27	–	8.79
NGC 300								
1	0.07	0.37	0.5	2.8	−0.52	0.25	1.75	8.91
2	0.11	0.28	0.6	5.0	−0.73	0.29	1.52	8.57
3	0.16	–	–	–	–	–	–	–
4	0.28	0.33	0.5	4.7	−0.83	0.22	1.41	8.60
5	0.33	0.34	2.4	6.3	−0.95	0.15	1.23	8.42
6	0.35	0.18	2.0	3.7	−0.58	0.15	1.25	8.77
7	0.39	0.30	3.2	5.5	−1.00	0.08	1.56	8.51
8	0.41	0.29	2.9	5.3	−0.86	0.12	1.25	8.54
9	0.48	–	–	–	–	–	–	–
10	0.53	0	6.0	7.8	−0.63	0.15	–	8.28
11	0.54	0.12	2.9	6.2	−0.91	0.14	1.23	8.44
12	0.55	0.26	2.3	7.3	−1.2	0.11	1.03	8.33
13	0.58	–	–	–	–	–	–	–
14	1.04	0.13	6.3	8.4	−1.4	0.03		8.27
15	1.05	0.14	5.6	8.5	−1.24	0.06	1.54	8.23
16	1.08	0.21	3.7	7.1	−1.5	0.04	–	8.35
NGC 7793								
Nucleus	0	–	0.8	3.5	−0.40	0.38	–	8.79
Nucl. W.	0.04	–	0.6	2.7	−0.47	0.25	–	8.96
34	0.20	–	0.4	2.8	−0.65	0.19	–	8.91
33	0.27	–	0.5	3.2	−0.58	0.28	–	8.83
36	0.31	0.61	2.1	5.6	−0.92	0.15	2.27	8.50
44	0.35	–	1.0	4.3	−0.65	0.26	–	8.66
25	0.35	0.26	1.4	4.1	−0.72	0.18	1.96	8.68
25N	0.35	0.30	1.4	4.9	−0.84	0.18	1.20	8.58
19 + 24 +26	0.37	–	0.9	4.0	−0.69	0.22	–	8.70
20	0.40	0.39	1.6	4.7	−0.75	0.19	1.52	8.61
20S	0.40	–	0.5	3.2	−0.62	0.23	–	8.83
13	0.51	0.53	1.1	5.6	−0.88	0.21	1.25	8.50

Table 5 – *continued*

Nebula	ρ/ρ_0	$C(H\beta)$	[O III]/ Hβ	[O II] + [O III]/Hβ	log [N II]/ [O II]	[N II]/Hα	[S II] 6717/ 6731	PES 12 + log O/H
13 S1	0.51	–	0.7	3.8	−0.40	0.43	–	8.73
13 S2	0.51	0.51	1.0	5.2	−0.82	0.22	1.75	8.54
10	0.63	0.19	0.9	5.1	−0.95	0.17	1.45	8.55
39	0.68	–	0.3	2.8	−0.56	0.24	–	8.91
4	0.78	–	2.1	8.6	–	–	–	8.23
2	0.82	0.34	2.4	6.7	−1.00	0.15	1.37	8.40
1	0.91	0.47	1.5	4.4	<−1.16	<0.07	–	8.66
133	0.99	0.18	3.3	6.2	<−1.23	<0.06	–	8.44
NGC 5236								
1	0.00	0.60	–	–	–	0.92	0.92	–
2	0.01	0.79	0.10	0.51	+0.66	0.65	0.83	9.72
3	0.01	–	–	–	–	0.83	0.99	–
4	0.02	–	–	–	–	0.67	1.30	–
5	0.02	0.96:	0.16	1.5	+0.08	0.55	1.10	9.30
6	0.20	0.50	<0.13	–	–	0.45	1.04	–
7	0.27	0.13	–	–	–	0.55	1.89	–
8	0.31	–	–	–	–	0.52	–	–
9	0.32	0.50	–	–	–	0.47	1.16	–
10	0.34	–	0.24	1.9	+0.05	0.67	1.33	9.18
11	0.35	0.79	<0.12	0.93	+0.12	0.43	–	9.50
12	0.36	0.39	–	–	–	0.57	–	–
13	0.36	0.75	0.26	2.0	−0.10	0.50	1.16	9.13
14	0.38	0.06	–	–	–	0.81	–	–
15	0.47	–	–	–	–	0.45	–	–
16	0.58	0.18	1.1	3.1	−0.10	0.55	1.37	8.85
17	0.58	–	–	–	+0.05:	0.46	2.8	–
18	0.65	–	–	–	–	0.58	–	–
NGC 5253								
1	0.01	0.13	5.9	7.8	−0.95	0.08	1.30	8.29
2	0.03	0.31	4.1	8.1	−1.15	0.10	1.47	8.27
3	0.04	0.23	8.5	9.7	−0.56	0.12	1.02	8.16
4	0.05	0.38	7.8	9.3	−0.77	0.09	1.08	8.18
5	0.05	0.11	4.6	8.1	−1.05	0.11	1.35	8.27
6	0.07	0.38	4.7	8.4	−1.12	0.10	1.30	8.26
7	0.12	0	5.3	7.6	−1.07	0.09	1.67	8.30
8	0.20	0.84	5.0	12.2	–	–	–	–

3.2 STRONG-LINE PROCEDURE (PES METHOD)

Pagel *et al.* (1980) provide a calibration of O/H from

$$\frac{[\mathrm{O\,II}] + [\mathrm{O\,III}]}{\mathrm{H}\beta}.$$

In Table 5 this O/H abundance is listed, along with a selection of the line strengths and other parameters of the nebulae.

The abundance variations against the radial distance with respect to the de Vaucouleurs radius ρ_0 (de Vaucouleurs, de Vaucouleurs & Corwin 1976) are shown for each galaxy in Fig. 2. Included in the figure are the results obtained by previous workers, analysed by the PES method. The scatter is substantial, as expected for a semi-empirical procedure, and we

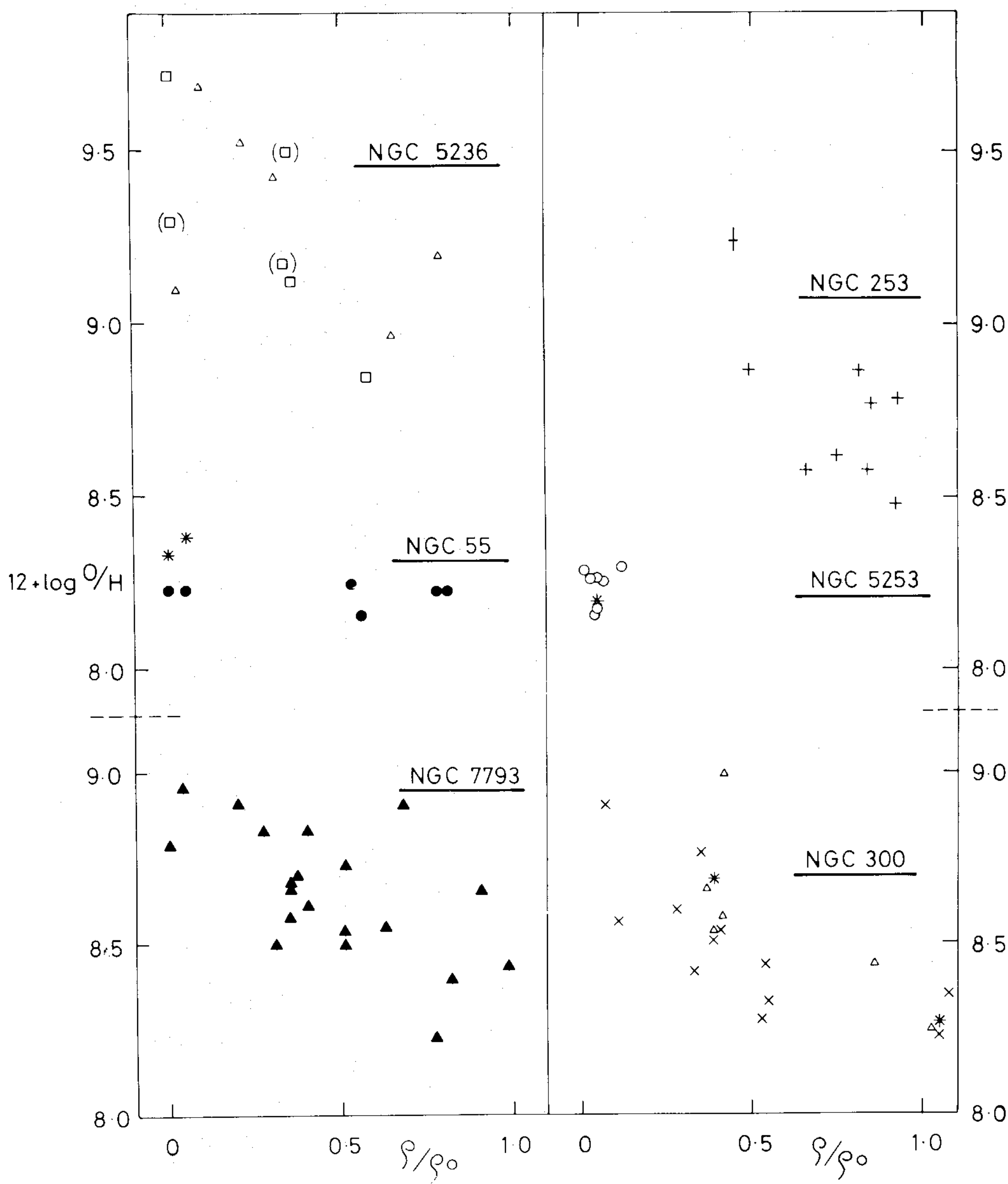

Figure 2. The oxygen abundance of the H II regions in each galaxy as a function of the normalized distance from the centre of that galaxy. △, observations by others, *, measured T_e.

conclude that it is necessary for a considerable number of H II regions to be observed before any detailed conclusions can be drawn. With the combined observations each of these galaxies except NGC 253 now has a respectable coverage.

It is worth mentioning that the phenomenon of weak [O III] and strong He I, which is interpreted (Searle 1971) as indicating high abundance in giant H II regions is present also among planetary nebulae. A study of one of these, which has a normal O/H but a high dust content, is in progress (Allen & Webster, in preparation).

4 Discussion of individual galaxies

4.1 NGC 55

NGC 55 has been classified as an edge-on Magellanic barred spiral, with the bar being almost end on (de Vaucouleurs & Freeman 1972), although the orientation makes classification very difficult. There is a bright emission complex in the direction of the bar and numerous H II regions throughout. Alloin & Sareyan (1974) have measured the brightest emission lines in the centre, but there have to our knowledge been no detailed studies.

Our work shows that the central H II region has an electron density $\sim 10^3\,\mathrm{cm}^{-3}$ and a high ionization level. In calculating the radial distance ratio ρ/ρ_0, this region has been taken as an arbitrary centre, and ρ_0 (= 15′.6) as the distance from this centre to the outermost contour visible on our plates in the direction eastward along the plane of the galaxy. The precise value of ρ/ρ_0 should not be taken too seriously, of course, because projection effects cannot be disentangled, but there is a clear separation between nebulae along the bar and those distant from it.

The result is that there is no radial gradient across NGC 55. The O/H ratio from the λ4363 method (12 + log O/H = 8.4) is slightly higher than from the strong-line method (8.23) and the former is the same as for nebulae in the LMC (also using the 4363 method, Pagel *et al.* 1978). The LMC has the same morphological type and is similar in size. The nitrogen abundance in NGC 55 (mean log N/O = −1.8) is one-half that in the LMC H II regions (−1.5) and generally lower than any other H II regions with a comparable oxygen abundance. This can be understood if nitrogen is partly a primary nucleosynthesis product (Edmunds & Pagel 1978) and if NGC 55 is either young or deficient in lower mass stars relative to the LMC.

4.2 NGC 253

NGC 253 is a large spiral with the suggestion of a central bar, evidence for non-circular motions (Pence 1978) and a nucleus with strong radio and infrared fluxes (Becklin, Fomalont & Neugebauer 1973, and others). Our observations of a region near the nucleus are too contaminated by the underlying starlight to give an accurate abundance, but limits on the strength of [O II] 3727 and [O III] 5007 and an estimate of c (= 2.4) from the Balmer lines gives a lower limit to the oxygen abundance of 12 + log O/H = 8.86. The two extended regions, Nos 2 and 3, near the nucleus probably have ionization conditions which differ from those of the giant regions assumed in Section 3.2. In the outer regions of NGC 253 the abundance lies between the giant M83 and the other Sculptor spirals. Further work should concentrate on nebulae in the inner part of this galaxy.

4.3 NGC 300

NGC 300 is a late-type spiral similar to M33 in appearance and mass, but with a larger hydrogen to total mass ratio than M33 (de Vaucouleurs & Page 1962). The luminosity distribution has been determined by de Vaucouleurs & Page (1962), but the zero point has not yet been established photoelectrically.

The abundances of six H II regions have been found by Pagel *et al.* (1979) and these have a gradient and absolute value very close to those in M33. Our further 13 values confirm their result and define a more precise relationship between abundance and radial distance. We have also been able to measure λ4363 in one of the inner H II regions, as well as two outer regions, thus showing the abundance gradient through the intrinsically more reliable abundance analysis.

Table 6. Surface brightness and abundance parameters.

Galaxy	r_e	a_e	μ_B	μ_B (corr)	Refs	(12 + log O/H)$_e$	Refs
NGC 253	3.2	6.4	22.0	22.0:	1	8.84	4
NGC 598 (M33)	9.8	12.1	22.8	22.7	2	8.55	5
NGC 1566	1.0	0.9	22.2	21.9	9	9.5	11
LMC	2.87	3.12	23.7	23.3	2	8.40	6
NGC 5194 (M51)	1.8	2.9	21.7	21.4	8	9.35	10, 5
NGC 5236 (M83)	2.1	2.2	21.5	21.1	3	9.23	4, 7
NGC 5457 (M101)	4.1	4.2	23.1	22.8	8	8.65	5
NGC 7793	1.8	2.1	22.2	22.3	2	8.67	4, 5

References

1. Pence (1978).
2. de Vaucouleurs & Davoust (1980).
3. Talbot, Jensen & Dufour (1979).
4. This paper.
5. Pagel & Edmunds (1981).
6. Pagel *et al.* (1978).
7. Dufour *et al.* (1980).
8. Okamura, Kanazawa & Kodaira (1976).
9. de Vaucouleurs (1973).
10. Dufour *et al.* (1980).
11. Hawley & Phillips (1980).

Explanation of headings

r_e — Equivalent radius. LMC in degrees, the others in arcmin.
a_e — Equivalent semi-major axis, LMC in degrees, the others in arcmin.
μ_B — The *B* surface brightness in magnitudes per square arcsec measured at r_e or a_e.
μ_B (corr) — μB corrected for inclination, internal absorption and galactic latitude. Corrections to NGC 253 are large.
(12 + log O/H)$_e$ — The mean value of 12 + log O/H measured at a galactocentric distance of a_e.

The nucleus of NGC 300 is very bright, red and almost unresolved. It has the unusual property of showing no Hα emission on our red scan and therefore of being normal! Two of the H II regions (Nos 7 and 11) have strong blue continua and broad He II λ4686 emission, and so are probably ionized by associations containing Wolf–Rayet stars. One of the nebulae (No. 11) is ring shaped and may fall into the class of W–R ring nebulae. NGC 300 may therefore be added to the select group of external galaxies in which W–R stars have been detected.

4.4 NGC 7793

NGC 7793 is the faintest of the five major galaxies in the Sculptor group (NGC 247 has not been included in our study) and is the prototype of the Sd type. Work on it is summarized by Davoust & de Vaucouleurs (1980). It has numerous H II regions and ionized hydrogen throughout the disc (Monnet 1971; Aguëro 1979). We find [O II] λ3727 on nearly all our spectra between the bright H II regions. The nucleus shows a composite spectrum with a contribution from red stars, nebular emission lines and a blue continuum with a strong Balmer jump, deep absorption lines of hydrogen and other fainter absorption lines (Fig. 1). The nuclear emission line strengths in Table 3 are badly affected by this absorption. Pagel & Edmunds (1981) refer to H II abundances in general agreement with ours.

4.5 NGC 5236 (M83)

M83 is a supergiant spiral, in the Centaurus Group and is a calibration object in the extragalactic distance scale. It has a hotspot nucleus, numerous H II regions in the disc and diffuse emission over much of the galaxy (Aguëro & Carranza 1980). The emission-line nucleus has been studied by Pastoriza (1975) and the abundance gradient has been found by Dufour *et al.* (1980) from six H II regions over the disc. Brand, Coulson & Zealey (1981) have measured some strong line ratios at 20 points.

Our work increases the number of abundance determinations by six. The gradient in O/H and the constancy in [N II]/Hα throughout the disc and its rise in the centre are confirmed. Fig. 2 shows clearly the need for a considerable number of observations when studying abundance gradients using only the strong lines since appreciable scatter is introduced by the statistical nature of the method of analysis. The reddening in this high abundance galaxy is generally somewhat higher than in the other galaxies studied (excluding NGC 253 which is highly inclined).

Probably the most useful extra information is on the nuclear region, since we were able to use a night of excellent seeing to isolate some of the individual knots or hotspots (see Plate 3). The spectrum of the underlying continuum varies from one knot to another; regions 1 and 4 are relatively blue with strong Balmer line absorption, the others are less blue with NaD absorption. The most striking differences between the nuclear and disc H II regions are first, the strong stellar contribution in the nucleus, second, the higher [N II]/Hα ratio in the nucleus and, third, the relatively high electron density implied by the [S II] ratio in the central hotspots, ($10^3\,cm^{-3}$ rather than $10^2\,cm^{-3}$ further out). This high density affects the abundance determination from strong line ratios in the sense that the abundances are underestimated. Even without allowance for a density effect, our accurate observations on region 2, close to the centre of the stellar component, and the lower precision (poor [O II] λ3727) on region 5, show that the abundance gradient of the disc probably continues monotonically into the nucleus. This is clear from the ([O II] + [O III])/Hβ ratio, from [O III]/Hβ and from the [O III]/[N II] ratio.

4.6 NGC 5253

NGC 5253 is classified as Irr IIp, and appears to consist of a stellar component with isophotal contours resembling an elliptical galaxy (Welch 1970), a neutral hydrogen component with a mass that would be expected for a lenticular or early spiral galaxy (Bottinelli, Gougenheim & Heidman 1972) and a striking complex of ionized gas (Evans 1952; Welch 1970, and others). The ionized gas, a surrounding cloud of clusters (van den Bergh 1980), two type I supernovae this century and fascinating, filamentary structure far out in the light of [O III] (Graham 1981), all argue for vigorous star formation over at least the last 10^8 to 10^9 yr, possibly triggered by interactions with M83. This makes the heavy element abundances of particular interest and in view of somewhat conflicting previous results (Welch 1970; Osmer, Smith & Weedman 1974), a redetermination of O/H and N/O is important.

We were fortunate again in having excellent seeing for our observations, so that individual knots in the central complex could be measured separately. None of the knots appeared to be anything other than normal H II regions. The electron temperature can be measured from [O III] in four of these regions and the strong-line method can be used for a further three. The abundance results are remarkably close for each method and for each of the seven nebulae, in spite of a fair spread in the O^{++}/O^{+} ratio. The O/H is about one-quarter that in Orion, but half way between the LMC and the SMC. The N/O ratio is not significantly different from N/O in Orion.

This is approximately the oxygen abundance expected for the underlying elliptical, based on the relation between absolute magnitude and [Fe/H] in ellipticals, and is also what is expected for either an elliptical or a type I irregular galaxy with the mass of NGC 5253. It is a lower abundance than expected for the m_H/m_{total} of a gassy irregular galaxy. It is a much lower abundance than in the regions of M83 that we have observed, but any gas being transferred to NGC 5253 from M83 would be expected to come from much greater radial distances where the O/H ratio is lower.

5 General discussion

The main purpose of this and previous work has been to search for the systematics of the abundance behaviour from one galaxy to another. No strong correlation with Hubble type or mass is apparent among the spirals (Pagel & Edmunds 1981) and the data in this paper. Comparison with the ratio of gaseous to total mass is more difficult, since only the global masses of H I are available for many of the galaxies and the percentage of ionized and particularly molecular gas is unknown, but probably considerable in many cases. The ratio of the H I mass to the total mass is not correlated with the abundance in these galaxies as it is among dwarf irregulars.

We find that the most significant galactic property in this respect may be the surface brightness of the stars. A characteristic surface brightness has been determined for each galaxy with both well-calibrated surface photometry and extensive measurements of the O/H ratio obtained from at least the [O III] + [O II] lines. This surface brightness is the mean *B* magnitude per square arcsec at the equivalent radius (r_e) or semi-major axis (a_e) (de Vaucouleurs & Page 1962) corrected for extinction within our Galaxy, inclination of the galaxy and for internal extinction. The relative corrections are large only for NGC 253 which has an inclination of 78°, a dusty appearance and emission from dust and molecules. An internal absorption based on $E(B-V)$ of $A_B = 1.50$ has been adopted (Pence 1978). The

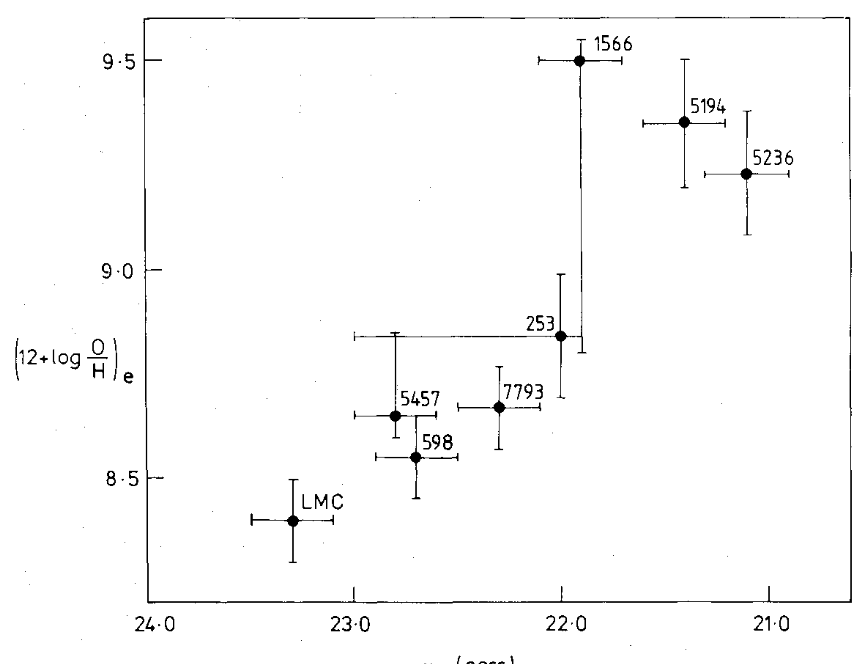

Figure 3. The relation for spiral galaxies between oxygen abundance in the interstellar medium and the corrected blue surface brightness of stars, each measured at the same characteristic distance from the galaxy centre.

bibliographic sources have been Davoust & Pence (1982) for the galaxy surface photometry and Pagel & Edmunds (1981) for the oxygen abundance. Galaxies with surface brightness calibrated only by rough estimates of the sky intensity have been omitted (NGC 300 and 1313), as has NGC 6946 for which the abundances have not been published in detail and which is at low galactic latitude. We have also excluded NGC 1365 in which the dominance of the bar and arms removes any semblance of radial symmetry.

In Fig. 3 the oxygen abundance at the characteristic radial distance (a_e) is plotted against the characteristic surface brightness. The error bars on the abundance reflect internal scatter between H II regions rather than calibration difficulties, and the errors in surface brightness have a contribution from the observations (taken as 0.1 mag) and a contribution from the corrections for extinction and inclination. The abundance in the Seyfert galaxy NGC 1566 depends on only one H II region at the appropriate radial distance.

A suggestive relation is obtained in the figure. This is the first strong correlation of abundances with a specific property of the discs of spiral galaxies and it is important that it be investigated further, perhaps by observing galaxies with the same Hubble type but different surface brightness.

To translate this new relation into the context of galactic evolution is hazardous without a knowledge of parameters like the column density of a gas and stars at each radius. In a closed system a simple model of chemical enrichment by succeeding generations of stars leads to a relation in which the heavy element abundance depends monotonically on the ratio of the residual gas to the total mass of the galaxy (Searle & Sargent 1972). Abundances in most of the small gassy irregulars do conform to this (Lequeux *et al.* 1979) though in the few well-studied spirals in which both abundances and gas/total mass are known as a function of radius, these quantities do not follow the expected relation (Lynden-Bell 1975). The relation involving the surface brightness of stars shown in Fig. 3 does not follow easily for a closed system. Rather, a scheme suggests itself in which the amount of gas in the disc is not determined by the number of preceding generations of stars, but is perhaps supplied continuously from a large source. The degree of enrichment could then depend on the sheer bulk of stars. Within a particular galaxy the dependence of O/H on surface brightness is less steep than the curve in Fig. 3, which would be expected if some radial mixing of gas occurs. This has already been suggested for barred spirals (Pagel *et al.* 1979). The general features implied by the abundance/surface brightness relation are thus akin to those of accretion models, which are successful in explaining the chemical statistics of old stars (e.g. Lynden-Bell 1975).

6 Conclusion

The six galaxies studied here illustrate most of the radial trends among H II region spectra which have become well known and increasingly well understood over recent years. In three of the galaxies (NGC 55, 300, 5253) reliable measurements of the O/H ratio have been possible because the faint [O III] λ4363 line has been detected. In the other three (NGC 253, 7793, 5236), where the indirect strong-line method has been used, it is clear that a large number of H II regions must be observed because of intrinsic scatter in the method and our results have contributed in this way.

Based on a small number of galaxies with suitable observational parameters, the characteristic abundance of a galaxy appears to be related most strongly to its characteristic surface brightness. This should be checked with more galaxies. If true, the relation implies that chemical evolution has not proceeded in a 'closed' system, but that some form of circulation or accretion has been operating.

Acknowledgments

It is a pleasure to thank Drs G. de Vaucouleurs, M. Edmunds, Professor B. Pagel, Drs W. Pence and A. Turtle for stimulating discussions and D. Malin for the production of the plates.

References

Agüero, E. L., 1979. *Astrophys. Space Sci.*, **65**, 423.
Agüero, E. L. & Carranza, G. J., 1980. *Astrophys. Space Sci.*, **70**, 251.
Alloin, D. & Sareyan, J-P., 1974. *Astr. Astrophys.*, **33**, 331.
Balick, B. & Sneden, C., 1976. *Astrophys. J.*, **208**, 336.
Becklin, E., Fomalont, E. & Neugebauer, G., 1973. *Astrophys. J.*, **181**, L27.
Bottinelli, L., Gougenheim, L. & Heidmann, J., 1972. *Astr. Astrophys.*, **17**, 445.
Brand, P. W. J. L., Coulson, I. M. & Zealey, W. C., 1981. *Mon. Not. R. astr. Soc.*, **195**, 353.
Brocklehurst, M., 1971. *Mon. Not. R. astr. Soc.*, **153**, 471.
Davoust, E. & de Vaucouleurs, G., 1980. *Astrophys. J.*, **242**, 30.
Davoust, E. & Pence, W. D., 1982. *Astr. Astrophys. Suppl.*, **49**, 631.
de Vaucouleurs, G., 1973. *Astrophys. J.*, **181**, 31.
de Vaucouleurs, G., 1979. *Astr. J.*, **84**, 1270.
de Vaucouleurs, G. & Page, J., 1962. *Astrophys. J.*, **136**, 107.
de Vaucouleurs, G. & Freeman, K. C., 1972. *Vistas Astr.*, **14**, 163.
de Vaucouleurs, G., de Vaucouleurs, A. & Corwin, H. G., 1976. *Second Reference Catalog of Bright Galaxies*, Texas. (U.T. Monographs in Astr. No. 2.)
de Vaucouleurs, G. & Davoust, E., 1980. *Astrophys. J.*, **239**, 783.
Edmunds, M. G. & Pagel, B. E. J., 1978. *Mon. Not. R. astr. Soc.*, **185**, 77P.
Dufour, R. J., Talbot, R. J., Jensen, E. B. & Shields, G. A., 1980. *Astrophys. J.*, **236**, 119.
Evans, D. S., 1952. *Observatory*, **72**, 164.
Graham, J. A., 1981. *Publ. astr. Soc. Pacif.*, **93**, 552.
Graham, J. A., 1982. *Astrophys. J.*, **252**, 474.
Hawley, S. A. & Phillips, M. M., 1980. *Astrophys. J.*, **235**, 789.
Lequeux, J., Peimbert, M., Torres-Peimbert, S., Rayo, J. F. & Serrano, A., 1979. *Astr. Astrophys.*, **80**, 155.
Lynden-Bell, D., 1975. *Vistas Astr.* **19**, 299.
Miller, J. S. & Mathews, W. G., 1972. *Astrophys. J.*, **172**, 606.
Monnet, G., 1971. *Astr. Astrophys.*, **12**, 379.
Okamura, S., Kanazawa, T. & Kodaira, K., 1976. *Publ. astr. Soc. Japan*, **28**, 329.
Oke, J. B., 1974. *Astrophys. J. Suppl.*, **27**, 21.
Osmer, P. S., Smith, M. G. & Weedman, D. W., 1974. *Astrophys. J.*, **192**, 279.
Osterbrock, D. E., 1975. *Astrophysics of Gaseous Nebulae*, W. H. Freeman.
Pagel, B. E. J., Edmunds, M. G., Fosbury, R. A. E. & Webster, B. L., 1978. *Mon. Not. R. astr. Soc.*, **184**, 569.
Pagel, B. E. J., Edmunds, M. G., Blackwell, D. E., Chun, M. S. & Smith, G., 1979. *Mon. Not. R. astr. Soc.*, **189**, 95.
Pagel, B. E. J., Edmunds, M. G. & Smith, G., 1980. *Mon. Not. R. astr. Soc.*, **193**, 219.
Pagel, B. E. J. & Edmunds, M. G., 1981. *A. Rev. Astr. Astrophys.*, **19**, 77.
Pastoriza, M. G., 1975. *Astrophys. Space Sci.* **33**, 173.
Pence, W. D., 1978. *Publication in Astronomy No. 14*, University of Texas.
Pradhan, A. K., 1976. *Mon Not. R. astr. Soc.*, **177**, 31.
Roberts, M. S., 1975. *Stars and Stellar Systems*, Vol. 9, p. 309. University of Chicago Press.
Rogstad, D. H., Lockhart, I. A. & Wright, M. C. H., 1974. *Astrophys. J.*, **193**, 309.
Sarazin, C. L., 1976. *Astrophys. J.*, **208**, 323.
Searle, L., 1971. *Astrophys. J.*, **168**, 327.
Searle, L. & Sargent, W. L. W., 1972. *Astrophys. J.*, **173**, 25.
Shields, G. A. & Tinsley, B. M., 1976. *Astrophys. J.*, **203**, 66.
Talbot, R. J., Jensen, E. B. & Dufour, R. J., 1979. *Astrophys. J.*, **229**, 91.
van den Bergh, S., 1980. *Publ. astr. Soc. Pacif.*, **92**, 122.
Welch, G. A., 1970. *Astrophys. J.*, **161**, 821.